frontiers in Physics

ORIGINAL RESEARCH
published: 29 October 2020
doi: 10.3389/fphy.2020.595971

Multiple Beam Laser Guidance for Patterning Irregularly Shaped Cells

Lucas Schmidt[1], *Zhonghai Wang*[1], *Xiaoqi Yang*[1], *Tong Ye*[1], *Thomas K. Borg*[2], *Yonghong Shao*[3]* *and Bruce Z. Gao*[1]*

[1]*Department of Bioengineering, Clemson University, Clemson, SC, United States,* [2]*Department of Regenerative Medicine and Cell Biology, Medical University of South Carolina, Charleston, SC, United States,* [3]*Key Laboratory of Optoelectronic Devices and Systems of Ministry of Education and Guangdong Province, College of Physics and Optoelectronics Engineering, Shenzhen University, Shenzhen, China*

Laser cell patterning is a distinctly effective technique for creating cell arrangements in culture that replicate *in vivo* tissue structure for studying contact-mediated cell-cell interactions. Conventional laser-based single-cell-manipulation techniques are limited by their inability to pattern irregularly shaped cells, such as rod-shaped cardiomyocytes. We report use of a spatial light modulator loaded with a computer-generated phase map to shape a single laser source into multiple laser-guidance beams distributed around the outer contour of an irregularly shaped cell to achieve accurate cell patterning. In addition to describing the principle and practice of the system design, we present what is to our knowledge the first achievement of patterning large, irregularly (rod) shaped adult rat cardiomyocytes in an end-to-end connected alignment to replicate the *in vivo* heart muscle cell connection without use of substrate surface modifications, which can interfere with in vivo-like cell-cell and cell-extracellular matrix interactions. Our research demonstrates that two-stage multiple beam laser guidance is effective: 1) A dual-beam configuration horizontally translates a cell from the outlet of the microfluidic cell delivery channel to a position above the cell deposition site and 2) A quad-beam configuration rapidly propels the cell axially through the suspension medium to the culture substrate with vertical movement of the cell patterning chamber. Our study reveals that 90% of the patterned cells maintained end-to-end connection 30 min after patterning, and mechanical junctions could be reinstalled between laser connected cells after overnight incubation. This demonstrates that multiple beam laser patterning is an outstanding tool for *in vitro* studying contact-mediated cell-cell interactions among irregularly shaped cells.

Keywords: optical force, multiple beams, cell patterning, cardiomyocyte, laser guidance

OPEN ACCESS

Edited by:
Michael W. Berns,
University of California, Irvine, United States

Reviewed by:
Anna Bezryadina,
California State University Northridge, United States
Ilia L. Rasskazov,
University of Rochester, United States

Correspondence:
Yonghong Shao
shaoyh@szu.edu.cn
Bruce Z. Gao
zgao@clemson.edu

Specialty section:
This article was submitted to Optics and Photonics, a section of the journal Frontiers in Physics

Received: *19 August 2020*
Accepted: *28 September 2020*
Published: *29 October 2020*

Citation:
Schmidt L, Wang Z, Yang X, Ye T, Borg TK, Shao Y and Gao BZ (2020) Multiple Beam Laser Guidance for Patterning Irregularly Shaped Cells. 8:595971. doi: 10.3389/fphy.2020.595971

INTRODUCTION

With conventional cell-culture techniques, the spatial control of single cells necessary to recreate the cell-cell contact arrangement found in native tissue is difficult. Since the development of Ashkin's optical force-based cell-manipulation techniques [1, 2], lasers have been used in microscopic applications to explore various biological interactions at the molecular and cellular levels [3, 4]. Research at the single cell and subcellular organelle levels involves laser trapping (using a laser-tweezer microscope) [5, 6] and laser guidance [7, 8]. Laser tweezer applications employ a high numerical aperture (NA) microscope objective to generate a strongly focused laser beam to 3D trap a

particle, such as a biological cell, within the beam's focal point. In laser guidance, a low NA microscope objective generates a weakly focused laser beam to simultaneously localize a particle to the beam axis and propel it in the beam-propagation direction.

With these principles, we developed a laser cell-micropatterning system in which the laser beam is focused in a transitional state between generating an optical trap and optical guidance [9]. Using this system, a single biological cell can be optically moved within a typical cell culture dish (e.g., 30 mm) and patterned into a predesignated cell culture microniche with very high spatial and temporal resolution [10–12]. However, this and the other currently available laser-based single-cell-manipulation techniques are limited by their inability to pattern irregularly shaped cells, such as rod-shaped cardiomyocytes.

To overcome this limitation, we used a spatial light modulator loaded with a computer-generated phase map to shape a single laser source into multiple laser-guidance beams, a procedure analogous to techniques used for holographic optical tweezers (HOT) [13, 14]. In contrast to HOT optical configurations, our system uses a low NA objective to produce multiple weakly focused laser-guidance beams positioned within the cell-micropatterning chamber. Using the detected cell shape from bright-field imaging, multiple beams can be distributed around the outer contour of an irregularly shaped cell to achieve accurate cell patterning. In addition to describing the principle and practice of the system design, we present what is to our knowledge the first achievement of patterning large, irregularly (rod) shaped adult rat cardiomyocytes in an end-to-end connected alignment to replicate the *in vivo* heart muscle cell connection without use of substrate surface modifications, which can interfere with in vivo-like cell-cell and cell-extracellular matrix interactions.

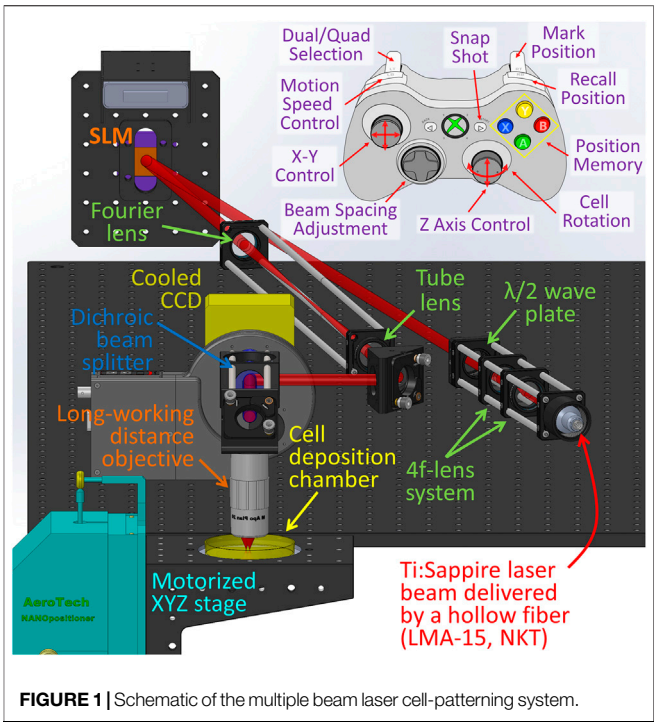

FIGURE 1 | Schematic of the multiple beam laser cell-patterning system.

MATERIALS AND METHODS

Cell Preparation

Adult cardiomyocytes were isolated from 4-week-old male Sprague–Dawley (SD) rats as described previously [15]. Briefly, SD rats were subcutaneously injected with heparin (5 units/g animal), anesthetized by inhalation of isoflurane (5%), and then euthanized following a protocol approved by Clemson University Institutional Animal Care and Use Committee. The heart was removed from the body through thoracotomy and immediately perfused through the aorta with warm calcium-free perfusion buffer (mM) (NaCl 113, KCl 4.7, KH_2PO_4 0.6 NaH_2PO_4 0.7, $MgSO_4$ 1.2, $NaHCO_3$ 12, $KHCO_3$ 10, HEPES 10, Taurine 30, BDM 10, Glucose 5.5) for 5 min. The heart was then digested continuously with enzyme solution (collagenase type II 0.8–1.0 mg/ml, trypsin 35 unit/ml, neutral protease 0.24 unit/ml, $CaCl_2$ 50 μM) for 40–45 min. During digestion, the calcium concentration of the enzyme solution was gradually increased to 500 μM by adding 100 mM $CaCl_2$ dropwise with an automatic syringe pump. Perfusion and digestion were conducted using a custom-made temperature-controlled perfusion system at 37°C. After digestion, cardiomyocytes were dissociated from minced ventricles by gentle mechanical agitation. Isolated cardiomyocytes were incubated at room temperature in perfusion buffer with 1,000 μM $CaCl_2$ for 15 min to finish the calcium reintroduction process and allowed to be precipitated by gravity during this time. The cell pellet was resuspended in culture medium (Dulbecco's modified Eagle's medium (Gibco), 2% fetal bovine serum (VWR), 5 mM creatine, 5 mM taurine, 5 mM sodium pyruvate, 2 mM L-carnitine, 10 mg Insulin-Transferrin-Selenium). Unless otherwise noted, all chemical reagents were purchased from Sigma-Aldrich. All enzymes were purchased from Worthington.

Multiple Beam Laser Cell-Patterning System Design

System Overview

Figure 1 illustrates a schematic of the multiple beam laser cell-patterning system, which was composed of several principal elements: laser guidance objective (×20 Mitutoyo Long Working Distance Objective), phase modulation spatial light modulator (Holoeye Pluto NIR-011), motorized 3-axis translation stage (Aerotech), and microfluidics-based cell-micropatterning biochip mounted in a cell deposition chamber that was equipped with a lab-built on-stage incubator (37°C and 5% CO_2).

The laser (2W Ti:Sapphire Spectra-Physics M3900-S laser tuned at 800 nm) was coupled to a large mode area hollow optical fiber (NKT photonics LMA-15) using a three axis optical fiber coupler stage (Thorlabs Max350D). The reason we chose the laser wavelength of 800 nm is because around this wavelength, the light absorption of both water and organic components of a cell, such as proteins and nucleic

acids, reach a relatively low level, and thus laser-cell damage can be kept minimum [16–18]. From the fiber, the laser beam was then collimated into the microscope via a fiber collimator (Thorlabs F810FC-780) to form an 8 mm-diameter beam and delivered to the SLM. A zero order $\lambda/2$ wave plate (Thorlabs WPH05M-808) was positioned before the SLM to match laser source polarization relative to the inherent liquid crystal polarization to optimize the intensities of generated first order diffraction beams. A 4f lens system was used to collect and resize the SLM-generated diffraction pattern. The first lens of the 4f system served as the Fourier lens, and the second one served as the tube lens in a conventional microscope. The focus ratio of the two lenses was selected in terms of the imaging objective (NA = 0.42) to ensure that the focal size (ω_0) of the laser beam was approximately 2 μm. In addition, the axial position of the tube lens was adjustable to match the focal plane of the multiple laser beams (having a wavelength of 800 nm) with the visible illumination light of the imaging system to be coplanar at the imaging CCD. This provided a clear image of the cell while trapped at the focal plane. A dichroic mirror positioned between the objective and the CCD (Photon Focus) allowed live imaging during optical manipulation through a collimated red LED light source (Thorlabs M625L3). The illumination beam was focused by a condenser on the imaging plane of the objective from below; this, with the objective and the CCD, formed a patterning microscope.

The cell patterning process was manually controlled using a joystick on an Xbox controller connected to the computer (**Figure 1**). Software was developed to synchronize the controller to the translational microscope stage so that the user could store the outlet position of the microfluidic cell-delivery channel: As cells were delivered out of the microfluidic channel, the multiple laser beam would trap a cell. The controller also stored the location where the cell was to be patterned and automatically moved the stage linearly between the outlet of the microfluidic channel and the cell patterning site at a preset speed. These Xbox controller functions were reported in our previous publication [10].

Microfluidics-Based Cell-Micropatterning Biochip

The microfluidic biochip served as a quasi-sealed chamber to 1) dispense cells near the laser patterning region and 2) dampen convection flow in the medium that would otherwise overpower and prohibit controlled optical manipulation of cells. The cell-micropatterning biochip was fabricated from polydimethylsiloxane (PDMS) using the techniques described in our prior publication [10]. The microfluidic channel cross-sectional area was 200 μm wide and 50 μm high to accommodate the transport of large cells. The microfluidic biochip was placed over the laser micropatterning site and syringe-injected (Normject 1 ml) through the cell reservoir with laser patterning medium (300 μL) to wet the PDMS microfluidic channels and fill the laser micropatterning chamber. Upon removal of the syringe, the cell inlet reservoir was filled with a cell suspension (60×10^3 cells ml^{-1}) to generate stable gravity-driven cell transport from the inlet reservoir to the microfluidic outlet outside the laser patterning region. From there, the laser beams were used to trap a cell and to guide it to the patterning region to be aligned and connected with the previously patterned cell.

SLM Multiple-Beam Generation

The SLM was composed of a 2D array (1,920 × 1,080 pixels 8.0 μm pitch) of individually addressable electro-optical elements capable of inducing discrete degrees (8-bit/256 levels) of phase modulation (up to 2.7π). The phase modulation of each element was controlled by the SLM driver through DVI (Digital Visual Interface) transmission of specially calculated data. When the data were transferred to the SLM, a computer-generated phase map was displayed. This phase map modulated the wave front of the incident laser beam to generate a phase-map-defined wave (e.g., multiple diverging beams), which was collected and focused into multiple focal points by a Fourier lens (f = 300 mm). To achieve dynamic cell guidance, we used a phase modulating SLM to generate the multiple laser beams with dynamically tunable foci for each irregularly cell shape.

The phase maps were computed using our lab-built iterative Fourier transform algorithm [19]. The positions of beams to be generated were specified by an array of points centered on a 2D plane that represented the focal, or Fourier plane. From these points, the phase map for generating the beams was computed using the iterative Fourier transform algorithm. Practically, once array spacing was determined, the phase maps were precomputed and stored in memory and recalled based on the Xbox controller joystick inputs, thus effectively removing the need for continuous recalculation. Upon memory recall, the corresponding phase map was transferred to the SLM driver over a standard DVI port on the GPU at a frame rate of 60 Hz.

Uneven power intensity might occur between the generated laser beams due to dissimilarities observed with each diffracted beam along its optical path and discrete pixilation effects incurred by the SLM. To address this issue, our pregenerated phase maps were optimized using a lab-developed algorithm so that the intensity between individual laser beams could be dynamically adjusted. Furthermore, to fully utilize the laser power, the generated phase maps combined zeroth and first order diffraction beam reflections so that laser intensity was not diminished by blocking the zeroth order diffraction (i.e., the direct reflection) beam. For example, if four beams were needed, then three beams were generated relative to the zeroth order beam.

Multiple Beam Foci Calibration

An in-microscope CCD beam profiling system using a 25 × 25 mm gold plated mirror (Thorlabs PFSQ10-03-M01) mounted to the motorized translational microscope stage was employed to image the generated laser beam array for software calibration based on the technique developed by Cogswell and coworkers [20]. The infrared cut-off filter positioned before the imaging CCD was replaced by a neutral density filter (ND-8.0) to attenuate the reflected signal. The airy disk for each holographic laser beam was imaged by scanning the mirror along the z-axis. The centroid of each imaged disk was identified and used to create a calibration matrix for correspondence between a computed diffraction pattern and

its resulting position within the objective field of view using the CCD pixel coordinates and z-axis stage position.

Neutral Buoyancy Laser Patterning Cell Culture Medium

To reduce the gravity driven cell-sedimentation rate, a high-density laser patterning medium was formulated to create a suspension of neutrally buoyant cells. An isotonic high-density solution (1.159 g/ml) was prepared by dissolving Histodenz (Sigma) in water (30% w/v) according to the manufacturer's instructions. This isotonic solution was then mixed with culture medium (1.0 g/ml) at different ratios to obtain laser patterning medium with densities ranging from 1.0 to 1.159 g/ml. Laser patterning medium with a density of 1.07 g/ml (1.066–1.075) significantly slowed the sedimentation rate of adult cardiomyocytes to about 1 μm/s, which made adult cardiomyocyte patterning easily achievable.

Large Irregular Cell Patterning

Optical-transport of cells from the outlet of the microfluidic channel to the patterning site was achieved by repositioning the 3-axis motorized translational stage relative to the laser beams focused by the stationary microscope objective. With respect to the laser propagation direction (axial direction) that was perpendicular to the horizontally placed cell-deposition chamber, movement occurred in the axial and transverse directions.

In a manner similar to our single beam laser patterning system, we used a low NA objective (NA = 0.42) to focus the laser beams with lower convergence angles than those used in a typical laser tweezers system to 1) optimize the optical force produced in both the axial and transverse directions and 2) increase the distance between the objective and the optically manipulated cell so that cell manipulation could be performed in a large volume such as in a cell culture dish. The optical force generated by a laser beam with various configurations on a curved interface such as the membrane of a biological cell has been analyzed in detail [9, 11, 21–24]. Consequently, we did not quantitatively analyze the forces here; rather, we explained our experimental design in terms of the known analytical results and our experimental observations about the generated optical force (e.g., the lateral components).

The first design consideration was that our optical system (i.e., the tube lens and the Fourier lens) was set up in such a way that multiple beams were focused in a transitional mode between typical laser tweezers and laser guidance [9]. For a strongly focused beam, both the axial and lateral components of the optical force point inward to the focal point, and thus the force can trap a biological cell in the focal point to form laser tweezers. For a weakly focused beam, the lateral components of the optical force also point inward to the focal point, but the axial component of the optical force is along the beam propagation direction. Consequently, in a weakly focused laser beam, a biological cell is simultaneously trapped radially and propelled to move along the beam axis. This phenomenon was first referred to as "particle guiding" by Ashkin [25, 26] when he used two opposing moderately diverging Gaussian beams to trap a particle. In this configuration, when one beam was blocked, he observed that the trapped particle was driven forward and guided by the second beam; he stated that the laser radiation pressure could achieve particle guidance. Since then, in a manner similar to laser tweezers, laser guidance (confinement of a cell on the beam axis and guiding it along the beam) has been used for cell manipulation [1, 27, 28]. Neither laser guidance nor laser tweezers has a clearly defined focus-condition. Our simulations of a spherical biological cell (15 μm in diameter) [9] indicate 1) when the waist (ω_0) of the focused laser beam (800 nm) is smaller than 2 μm, a laser tweezer is formed; 2) when ω_0 = 4 μm, laser guidance is formed without axial confinement forces toward the beam focal point; 3) when ω_0 = 2 μm, a transitional mode between laser guidance and laser tweezers is formed, in which the axial trapping effect (tweezers mode) is generated only in the longitudinal sections near the beam focal point; elsewhere, the axial forces point in the laser propagation direction (guidance mode) [9]. As we noted earlier herein, this transitional mode provides not only sufficient radial trapping force (laser tweezers) for cell capture, but also the necessary force range (laser guidance) for laser navigation with the trapped cell.

Our previous experiments showed that when a single beam was used to trap one end of an adult cardiomyocyte, the cell tended to rotate to align its longitudinal axis with the laser beam, hindering fine adjustment of cell alignment. To trap the cell in a position in which its long axis remained in a horizontal plane, at least two laser beams should be used. Our experiments reported here demonstrated that a two-beam configuration could achieve precise placement and alignment of adult rat cardiomyocytes with end-to-end contact as observed in cardiac tissue. In general, two laser beams positioned equidistantly from the lateral axis that bisects a cell body (**Figure 2A**) were respectively focused at the two ends of the cell. A typical adult cardiomyocyte is about 80–120 μm long with a diameter in the range of 15–25 μm. As shown in **Figure 2B**, a laser beam focused at one end of the cell could be selectively positioned at two possible sites. When positioned at the longitudinally flattened region (Focal site 1), the major optical forces exerted on the cell would be a lateral trap. When the beam was at the end edge (Focal site 2), in addition to the lateral trap forces (F_T) there was a longitudinal pulling force (F_L). When the two beams were respectively positioned at each end edge, the resulting optical force trapped the cell horizontally with the longitudinal axis of the cell passing the two focal points. In this situation, due to the typical cell shape, the longitudinal components of the forces (i.e., the stretch forces) generated by the two laser beams were against each other, while the lateral components were parallel with each other along the same direction. Consequently, with this dual beam configuration (dual beam trapping mode), we could guide the rod-shaped cardiomyocytes to move laterally (**Figure 2A**) instead of longitudinally. To achieve longitudinal movement of a cell to decrease flow resistance, the distance between the two beams was decreased (dual beam guidance mode). Subsequently, when the two beams were positioned closer along the longitudinal axis of the cell, the leading beam (at the front) generated Focal site 2 type

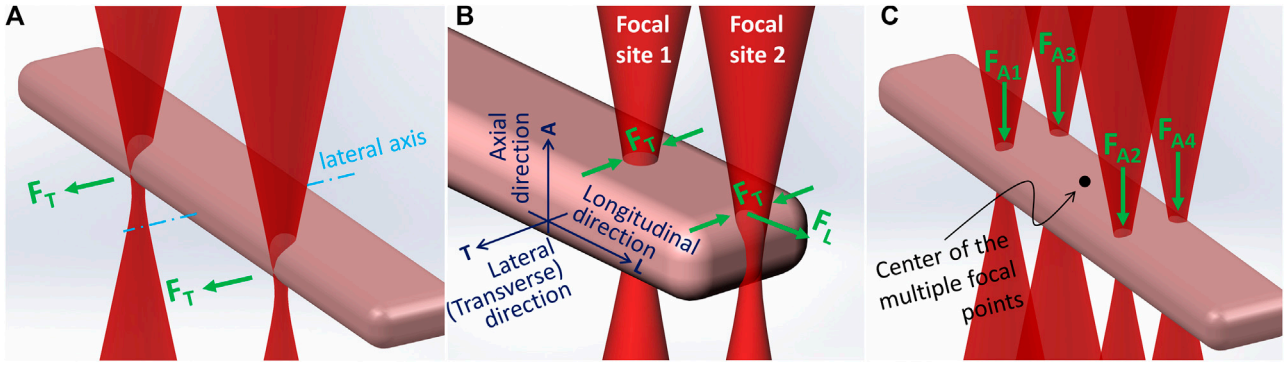

FIGURE 2 | Configurations of the multiple laser beams and the major optical forces generated.

forces, providing the longitudinal guidance force, and the trailing beam generated Focal site 1 type forces without inducing an opposing longitudinal force. When using the dual beam trapping mode, the two beams could be used to rotate the cell around the axial axis that passed through the center of the cell. This rotation was achieved by rotating the phase map, which was used to generate the dual beams, incrementally at 5° angle steps using the Cell Rotation button on the Xbox controller. The two operations just described are typically used to achieve fine adjustment at the final stage of placing a cell to form an end-to-end cell connection.

Practically, at the beginning of the laser patterning process, the stage was manually controlled using the Xbox controller joysticks to move so that the outlet of the microfluidic channel and the site where a cell was to be patterned were consecutively centered on the screen. The corresponding coordinates were stored by first holding the Mark Position button and then the desired Position Memory buttons (A, B, X or Y, four positions that could be memorized). A similar function was programmed to recall a position using the Recall Position and Position Memory buttons. Due to the limited field of view provided by the objective, these features were necessary to store the patterning site and quickly return to the outlet of the microfluidic channel and vice versa. The distance between the two sites was typically more than several millimeters and could never be visualized in the same screen during the patterning procedure.

Regardless of where the stage was moved to, the laser beam remained stationary in the live imaging field of view. Because IR (infrared) filters were used in the imaging system, the multiple laser focal points could not be seen. An in-house method to find the focus of the laser beam, which was also used to achieve the coplanarity of the laser's focal plane and the imaging system's object plane, was to use the two laser beams to burn two mediumdents on a black paper that was placed on the stage; the dents were then marked on the screen using a colored pencil, which signposted the center of the multiple focal points (**Figure 2C**). To begin patterning, the stage was moved to the outlet of the microfluidic channel in the vicinity of the focal point marker on the screen. When cells were visually observed leaving the outlet, a cell was selected. By pushing the Snap Shot button on the Xbox controller, an image of the cell was acquired. Immediately, the cell contour was traced to determine the space parameters for the dual- and quad-beam configurations, which were saved and could be recalled by using the Dual/Quad Selection button. The dual beam trapping mode was selected first to trap the cell. Then, the cell patterning site was recalled, and the cell was moved toward the site. Determined by the practical situation (e.g., the convection flow and cell shape), either lateral or longitudinal movement could be used, and the moving speed was adjusted manually using the Motion Speed Control button (e.g., ±10 μm/s per step).

When the cell was moved by laser from the outlet of the microfluidic channel to a position above the cell patterning site using the dual-beam configuration, the quad-beam configuration, shown in **Figure 2C**, was selected to guide the cell down through the medium and onto the culture substrate. Meanwhile, the chamber (controlled via the *Z*-Axis Control button) was moved up to increase the cell deposition speed. In the quad-beam configuration, laser beams passed through the cell edge curvature and thus experienced concentrated scattering effects; the beams therefore imparted more axial propulsion to the cell. With beams positioned around the contour, the antagonistic optical force confined the cell within the beam-array while maintaining beam positions along high curvature regions to achieve peak axial force. After the cell was pushed to be landed on the substrate, the dual-beam configuration was used to fine tune longitudinal alignment to achieve end-to-end connection.

RESULTS

Generation of the Holographic Multiple Laser Beams

For patterning adult cardiomyocytes, dual- and quad-beams were generated. For dual-beam configuration, we designed a phase map that generated a single first-order diffraction beam with the zeroth-order beam forming the second beam. By selecting various grating constants, a sequence of phase maps corresponding to dual-beam configurations with varying beam spacing were generated and stored in the memory to be uploaded to the SLM when needed. For quad-beam configuration, phase maps

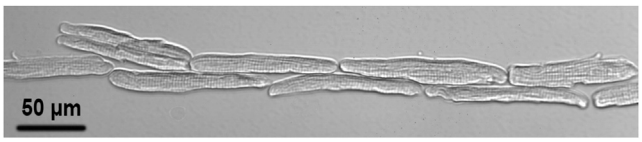

FIGURE 3 | A typical laser patterned adult cardiomyocyte culture imaged with the patterning microscope after 30 min culture in the on-stage incubator upon completion of the pattern.

for generating three first-order diffraction beams were designed. To properly share optical intensity between the zeroth and first order beams, the polarization status of the incident beam was adjusted prior to laser patterning. This allowed us to control the power distribution between the 0th and 1st order. This adjustment, however, did not provide absolute control over the power at each beam spot for the quad-beam configuration: The power uniformity at each first order spot also depends on the algorithm used to generate the phase map. Because the cell-shape and -size variations were not dramatic, we adjusted the phase map with various polarization states to find an optimal phase map for the beam configuration with the averaged beam distances and used it in the experiment. The actual difference among the beams was less than 5%. The typical intensity for each beam used in our experiments was 100 mW for the dual-beam configuration and 50 mW for the quad-beam configuration, measured after the objective. Focal point intensity plots, produced by plotting laser intensity along a line intersecting first order airy disk centroids, were used to measure the laser beam waists (ω_0). Plots were normalized and evaluated using the transverse distance between laser intensity points at $1/e^2$ of the maximum. Beam waist measurements were approximately 2 μm.

Using the GLMT simulation technique, we obtained a simulated optical force on the order of 10 pN exerted on a 20-μm diameter (spherical shape) neonatal cardiomyocyte in the laser patterning medium described in this paper. This simulation used the same laser beam employed in the research reported here: a 200 mW and 800 nm laser beam focused with ω_0 equal to 2 μm [9]. Practically, we could laterally move a 20-μm spherical neonatal cardiomyocyte with a constant speed of 50 μm/s using a laser beam of the same parameters in the same laser patterning medium. By using the Stokes drag force formulas, we could estimate that the drag force is about 10 pn. Using a laser with the same parameters as were just described and in the same laser patterning medium, we could trap one end of a typical rod-shaped adult cardiomyocyte and pull the cell along its longitudinal orientation with a speed of 50 μm/s [29] although we could not flexibly control its orientation. Thus, we can estimate the drag force of such an irregularly shaped cell to be similar to a spherical cell with a diameter of 20 μm, which we could move with a speed of 50 μm/s. The experimental data we report here showed that we could use a multiple beam to move a typical adult myocyte laterally, although the drag force might be a little higher than the longitudinal movement. Actually, we did not fill the entire back entrance of our 0.42 NA objective, otherwise, the waist size should be smaller than 2 μm, which might decrease the range of the optical force as we discussed previously [9].

End-To-End Alignment of Irregularly Shaped Adult Rat Cardiomyocytes

Supplementary Movie S1 shows a typical dual beam lateral guidance of the rod-shaped cardiomyocyte with a maximum guidance speed of approximately 30 μm/s. **Supplementary Movie S2** shows a typical dual beam longitudinal guidance with a maximum guidance speed of approximately 50 μm/s. Axial laser guidance was achieved using a quad-beam configuration around the cell contour with a maximum guidance speed of approximately 30 μm/s. **Figure 3** shows a typical pattern imaged using the patterning microscope.

A roughly 1.0°C/100 mW temperature increase has been report in a laser tweezers study using a 1,064 nm CW laser with no observable DNA damage or changes in cellular pH levels [30]. We experimentally estimated the absorption coefficient for freshly isolated neonatal cardiomyocytes to be 0.039 mm^{-1} (at 800 nm) using opal glass transition spectrophotometry [31]. However, this technique cannot completely compensate for sample scatter and so measured values may be 2 to 10 times larger than their true values [31]; when taking this into consideration our measured values of absorption coefficient for cardiomyocytes are likely between 0.004 and 0.02 mm^{-1}. These values appear to agree with a cardiac tissue absorbance (λ = 660 nm) of 0.006 mm^{-1} reported by Costantino and coworkers [32].

With the cell having an absorption coefficient estimated in our experiments for the wavelength we used (800 nm), there was no noticeable optical absorption of the laser patterning medium at this power level (200 mW). When there was a significant degree of absorption, the medium typically begins to heat and creates strong convection currents. Because we did not see this effect (e.g., **Supplementary Movies**), we extrapolated that there was

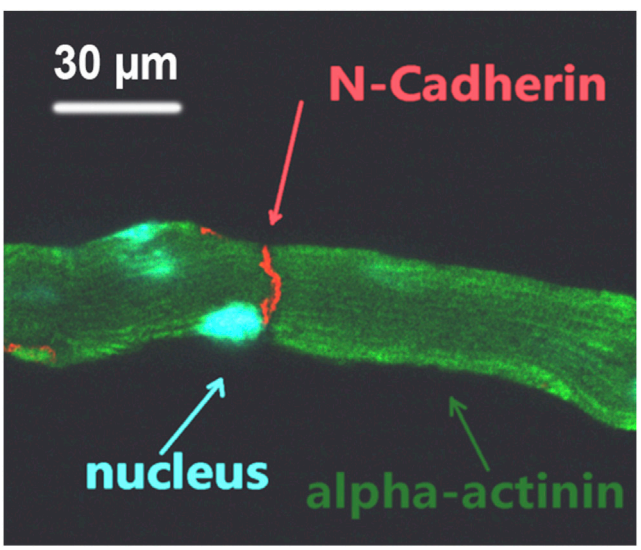

FIGURE 4 | Triple-stained fluorescence image of laser patterned adult cardiomyocytes; the formation of mechanical connection between end-to-end connected cells is indicated by N-cadherin.

minimal laser-medium and laser-cell (a single cell in suspension is transparent) heating. Further, a weakly focused beam was typically placed on the edge of a cell, away from subcellular components; there, the heating effect could be passively cooled by the surrounding medium in the chamber we used, which had a diameter of approximately 20 mm.

Mechanical Coupling Between End-To-End Connected Adult Rat Cardiomyocytes

Supplementary Movie S3 shows the synchronized contraction of three laser patterned cardiomyocytes; their dynamic connection indicated the formation of mechanical connection between the patterned cells. This movie was recorded using the patterning microscope 30 min after completion of patterning. To further confirm the mechanical connection after laser patterning, the patterned cell cultures were removed from the patterning system and placed into a conventional incubator to culture overnight. The culture was then fixed and immunofluorescence stained for cell nucleus, z disk, and N-cadherin. **Figure 4** shows a typical fluorescence image of the stained pattern; the formation of mechanical junction is indicated by N-cadherin staining.

DISCUSSION

Cardiac-muscle tissue is composed of many interlocking cardiomyocytes: Each cardiomyocyte expresses a rod-shaped morphology, as depicted in Borg's publication [33], and contracts along its longitudinal axis. All cardiomyocytes in the heart are connected end-to-end, forming a synchronously contracting network to pump the blood in the entire body through the heart in less than a minute, as illustrated in Figure 4.3 in Dr. Donald Longmore's book [34]. At the interface of connected cardiomyocytes is a region known as intercalated disks, which contain 1) tight junctions between the cardiomyocytes to prevent cell separation during cell contraction and 2) gap junctions to allow electrochemical signals to pass rapidly so the cardiac muscle tissue can be triggered simultaneously. Many heart diseases are related to structural changes of the cardiac muscle. Due to the complexity of *in vivo* cardiac muscle tissue, progress in development of new knowledge on how structural changes in cardiac muscle tissue affect heart function is heavily dependent on culture of adult cardiomyocytes. Although adult cardiomyocytes are known to be the most in vivo-like model for study of cardiac muscle, they rapidly dedifferentiate, losing their in vivo-like phenotype in culture [35]. Many efforts have been made to maintain the in vivo-like phenotype of adult cardiomyocytes by forming end-to-end cell connections among adult cardiomyocytes in culture, including mechanical stretching and magnetic alignment. Our laser cell-micropatterning technique has demonstrated the potential to achieve end-to-end cell connection [29]. Our previous technique, for cell guidance, used only a single laser beam. Although it could move large irregular cells, controlling cell orientation prior to patterning on a culture substrate was difficult due to the nonuniform hydrodynamic and optical

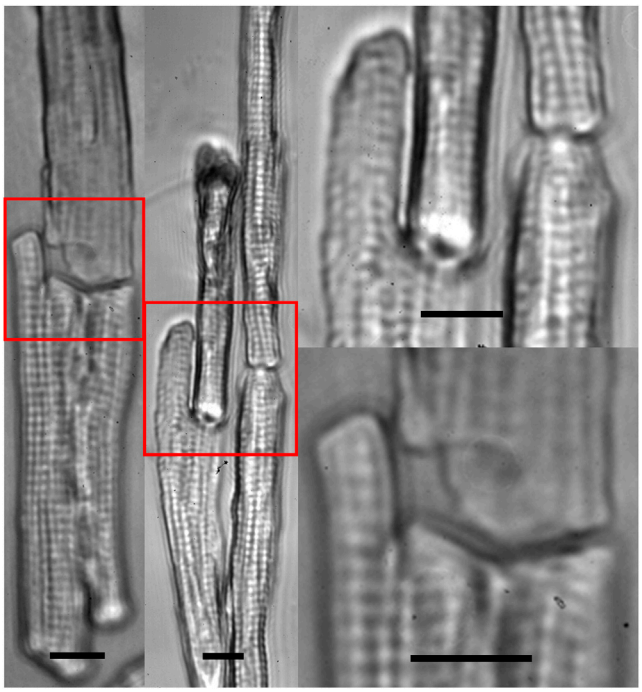

FIGURE 5 | Zoom-in images of multiple beam-patterned adult cardiomyocytes with end-to-end intercellular connections in culture in the on-stage incubator imaged with the patterning microscope 30 min after completion of the pattern (scale bars = 10 μm).

forces cells experience during laser patterning: Viscous drag around the irregularly shaped cell body affects its 3D orientation during optical guidance in the laser patterning medium during transit from the cell injection biochip to the point where the cell is pushed to the culture substrate. Particularly during low translational velocities, the rod-shaped cell body experienced optical forces that attempted to align its long axis with the beam propagation direction. This axial orientation (vertical to the cell substrate and the imaging plane), in addition to resisting cell movement, made difficult the final end-to-end alignment of the guided cell with the previously aligned cell. Use of multiple laser beams provides the ability to control cell orientation relative to the axis of patterned cells. Because the cell body is kept level with the substrate and the imaging plane, its long axis is completely in focus before deposition. Therefore, orientation of a cell's long axis is controlled by the torque induced across the cell body from multiple optical forces along the length of the cell.

Our research demonstrated that two-stage multiple beam laser guidance is effective: It allows 1) the horizontal translation of a cell from the outlet of the microfluidic cell delivery channel to a position above the cell deposition site without vertical movement of the cell patterning chamber and 2) the rapid axial propulsion of the cell in suspension to the culture substrate. During horizontal translation, a dual beam configuration laterally pulls the cell above the site of deposition. When the guided cell is positioned over the laser patterning site, a quad-beam configuration propels, or guides, the cell to the culture substrate as depicted in **Figure 2**. Due to the

inherent shape of cells, their outer edges produce the maximum optical force resulting from increased light diffraction at high curvature boundaries. By adaptively positioning the laser beams along the cell contour, the imparted optical force is controlled and maximized. With a single beam divided into multiple first order beams, optical intensity is shared among all generated beams. Generating more or fewer beams around the cell contour decreases or increases the beam power, respectively. The dynamic and controlled optical-force distribution along a cell body defines its resulting orientation within the beam matrix. When multiple beams are used, irregular cell bodies experience an induced optical torque in the form of roll, pitch, and yaw. Our research concludes that two beams for laterally moving the cell and four beams to guide cell down to the substrate are the optimal selection of the beam number.

Our previous study [15] suggested that breaking of intercalated discs caused force imbalance on both sides of the Z-discs adjacent to the cell ends, which played an important role in the dedifferentiation accompanied by sarcomeric dissociation in freshly dissociated adult cardiomyocytes. Consequently, our intention here was to use multiple laser beams to restore cell-cell connection. Our data (**Figure 4**) demonstrated that mechanical junctions could be reinstalled between laser connected cells. In **Figure 5**, cell manipulation-accuracy is seen at the submicron level [36]; laser guidance achieved even end-to-end connection between cells with irregular interfaces. Although our study revealed that 90% of the patterned cells maintained end-to-end connection 30 min after patterning, when a single cell in a set of patterned cells started to contract, it could become disconnected from the neighboring cells, as shown in **Figure 3** (i.e., the lower right cell). But, when we triggered patterned cells to contract synchronously, they were observed to remain connected (data not shown). This and our other studies on adult cardiomyocyte culture stimulated us to hypothesize that, in addition to end-to-end connection, two other conditions must be met to enable adult cardiomyocytes to preserve their sarcomeric structures: 1) 3D gel culturing environment and 2) constant electrical triggering. Systematically studying these conditions is our future work.

We present the use of multiple beam laser guidance to accurately laser pattern large irregularly shaped cells, which are traditionally too big and cumbersome to pattern using single beam systems. Multiple beam patterning techniques provide a higher degree of control during laser patterning by applying optical forces at key points along the cell contour for optimal force distribution. For the application of patterning adult cardiomyocytes, only in-plane translation and rotation are required. For the general application of manipulating irregularly shaped cells, each focal point of the multiple beams can be individually shifted axially to generate a torque with respect to a horizontal axis to tilt the cell. For producing a torque, the phase map for creating multiple beams focused on different axial locations can be generated by using an array of points centered on a 2D plane of defined inclination with respect to the horizontal plane. **Supplementary Movie 4** shows five-beam guidance of five neuronal cells. Because the laser beams are invisible, to demonstrate multiple beam manipulation, it is better to use individual spherical cells trapped by different beams than to use a single large cell. The movie demonstrates that, in addition to in-plane translation of the cells and rotation of the outside four cells relative to the center cell, the four outside cells can be moved axially out of the plane where the center cell is trapped.

While multiple beam laser patterning is suitable for studying cell-cell interactions that require very high temporal and spatial resolution, the technique is nevertheless incapable of construction of tissues composed of thousands of cells, vasculature and extracellular matrix. Laser patterning requires constant user input; therefore, the time required to recreate large multicellular tissues depends on a user's proficiency and availability.

CONCLUSION

The single-cell laser patterning of large irregularly shaped cells was demonstrated using adult cardiomyocytes, which we aligned end-to-end at the single cell level by incorporating techniques used by multiple beam optical force microscopes. Our continued research in the utility of laser-guidance has realized a valuable tool in creating spatially configured cell cultures by providing increased control and patterning rates in comparison to conventional laser tweezers.

DATA AVAILABILITY STATEMENT

The datasets presented in this study can be found in online repositories. The names of the repository/repositories and accession number(s) can be found in the article/ **Supplementary Material**.

ETHICS STATEMENT

The animal study was reviewed and approved by Clemson University Institutional Animal Care and Use Committee (protocol number AUP2017-069 and AUP2016-042).

AUTHOR CONTRIBUTIONS

LS designed the system, ran the experiment, organized the results, and constructed and wrote the manuscript. ZW ran parts of the experiment. XY prepared the adult cardiomyocytes and conducted the cell culture. TY wrote the SLM program. TB guided the biological study of the adult cardiomyocytes. YS supervised the optical system design and data acquisition and analysis and revised the manuscript. BZG supervised the authors starting from the study of the principle through experimental design and finalization of the paper.

FUNDING

This study was partially supported by National Institutes of Health through SC COBRE (P20RR021949 and P20GM130451), R01 funding (R01HL124782 and R01HL144927); National Natural Science Foundation of China (61775148); and the National Science Foundation EPSCoR Program (OIA-1655740).

ACKNOWLEDGMENTS

We thank Michael Zile and Catalin Baicu from Medical University of South Carolina for assistance with rat adult cardiomyocyte dissection.

SUPPLEMENTARY MATERIAL

The Supplementary Material for this article can be found online at: https://www.frontiersin.org/articles/10.3389/fphy.2020.595971/full#supplementary-material

REFERENCES

1. Ashkin A. History of optical trapping and manipulation of small-neutral particle, atoms, and molecules. *IEEE J Sel Top Quant Electron* (2000) **6**(6): 841–56. doi:10.1109/2944.902132.
2. Ashkin A, Dziedzic JM, Bjorkholm JE, Chu S. Observation of a single-beam gradient force optical trap for dielectric particles. *Opt Lett* (1986) **11**(5):288–90. doi:10.1364/ol.11.000288.
3. Grier DG. A revolution in optical manipulation. *Nature* (2003) **424**(6950): 810–6. doi:10.1038/nature01935.
4. Berns MW, Wright WH, Steubing RW. Laser microbeam as a tool in cell biology. *Int Rev Cytol Surv Cell Biol* (1991) **129**:1–44. doi:10.1016/s0074-7696(08)60507-0.
5. Svoboda K, Block SM. Force and velocity measured for single kinesin molecules. *Cell* (1994) **77**(5):773–84. doi:10.1016/0092-8674(94)90060-4.
6. Wright WH, Sonek GJ, Tadir Y, Berns MW. Laser trapping in cell biology. *IEEE J Quant Electron* (1990) **26**(12):2148–57. doi:10.1109/3.64351.
7. Odde DJ, Renn MJ. Laser-guided direct writing for applications in biotechnology. *Trends Biotechnol* (1999) **17**(10):385–9. doi:10.1016/s0167-7799(99)01355-4.
8. Odde DJ, Renn MJ. Laser-guided direct writing of living cells. *Biotechnol Bioeng* (2000) **67**(3):312–8 doi:10.1002/(sici)1097-0290(20000205)67:3<312::aid-bit7>3.0.co;2-f.
9. Ma Z, Liu Q, Yang H, Runyan RB, Eisenberg CA, Xu M, et al.. Laser patterning for the study of MSC cardiogenic differentiation at the single-cell level. *Light Sci Appl* (2013) **2**:e68. doi:10.1038/lsa.2013.24.
10. Borg N, Schmidt L, Qin W, Yang XQ, Lin YL, DeSilva MN, et al.. Microfluidics-based laser cell-micropatterning system. *Biofabrication* (2014) **6**(3):035025. doi:10.1088/1758-5082/6/3/035025.
11. Ma Z, Pirlo RK, Wan Q, Yun JX, Yuan XC, Xiang P, et al. Laser-guidance-based cell deposition microscope for heterotypic single-cell micropatterning. *Biofabrication* (2011) **3**(3):0341071–8. doi:10.1088/1758-5082/3/3/034107.
12. Pirlo RK, Ma Z, Sweeney A, Liu HH, Yun JX, Peng XA, et al. Laser-guided cell micropatterning system. *Rev Sci Instrum* (2011) **82**(1):193–217. doi:10.1063/1.3529919.
13. Padgett M, Di Leonardo R. Holographic optical tweezers and their relevance to lab on chip devices *Lab Chip* (2011) **11**(7):1196–205. doi:10.1039/c0lc00526f.
14. Dufresne ER, Spalding GC, Dearing MT, Sheets SA, Grier DG. Computer-generated holographic optical tweezer arrays. *Rev Sci Instrum* (2001) **72**(3): 1810–6. doi:10.1063/1.1344176.
15. Liu H, Qin W, Wang Z, Shao Y, Wang J, Borg TK, et al. Disassembly of myofibrils and potential imbalanced forces on Z-discs in cultured adult cardiomyocytes. *Cytoskeleton* (2016) **73**(5):246–57. doi:10.1002/cm.21298.
16. Gao TN, Owens S, Bakken D, Gao BZ. Cell viability test after laser guidance. *Prog Biomed Opt Imaging* (2006) **7**(7):608418. doi:10.1117/12.651467.
17. Tuchin VV. *Tissue optics: light scattering methods and instruments for medical diagnostics*. 3rd ed. Bellingham, WA: SPIE (2015)
18. Kong XD, Cruz GMS, Silva BA, Wakida NM, Khatibzadeh N, Berns MW, et al. Laser microirradiation to study in vivo cellular responses to simple and complex DNA damage. *J Vis Exp* (2018) **131**:61–74. doi:10.3791/56213.
19. Ma B, Yao B, Li Z, Lei M, Yan S, Gao P, et al.. Generation of three-dimensional optical structures by dynamic holograms displayed on a twisted nematic liquid crystal display. *Appl Phys B* (2013) **110**(4):531–7. doi:10.1007/s00340-012-5289-x.
20. Dan CJ, Sheppard CJR, Moss MC, Howard CV. A method for evaluating microscope objectives to optimize performance of confocal systems. *J Microsc* (1990) **158**:177–85. doi:10.1111/j.1365-2818.1990.tb02991.x.
21. Ashkin A. Forces of a single-beam gradient laser trap on a dielectric sphere in the ray optics regime. *Methods Cell Biol* (1998) **55**:1–27. doi:10.1016/s0091-679x(08)60399-4.
22. Nahmias YK, Zhi Gao B, Odde DJ. Dimensionless parameters for the design of optical traps and laser guidance systems. *Appl Optic* (2004) **43**(20):3999–4006. doi:10.1364/ao.43.003999.
23. Nahmias YK, Odde DJ. Analysis of radiation forces in laser trapping and laser-guided direct writing applications. *IEEE J Quant Electron* (2002) **38**(2):131–41. doi:10.1109/3.980265.
24. Lock JA. Calculation of the radiation trapping force for laser tweezers by use of generalized Lorenz–Mie theory II on-axis trapping force. *Appl Optic* (2004) **43**(12):2545–54. doi:10.1364/ao.43.002545.
25. Ashkin A, Dziedzic JM, Yamane T. Optical trapping and manipulation of single cells using infrared laser beams. *Nature* (1987) **330**(6150):769–71. doi:10.1038/330769a0.
26. Ashkin A. Acceleration and trapping of particles by radiation pressure. *Phys Rev Lett* (1970) **24**:156–9. doi:10.1103/physrevlett.24.156.
27. Jonás A, Zemánek P. Light at work: the use of optical forces for particle manipulation, sorting, and analysis. *Electrophoresis* (2008) **29**(24):4813–51. doi:10.1002/elps.200800484.
28. Dholakia K, Lee WM. Optical trapping takes shape: the use of structured light fields. *Adv Atom Mol Opt Phys* (2008) **56**:261–337. doi:10.1016/s1049-250x(08)00015-3.
29. Ma Z, Pirlo RK, Yun JX, Peng XA, Yuan XC, Gao BZ. Laser guided-based cell micropatterning. In: BR Ringeisen, BJ Spargo, PK Wu, editors *Cell and organ printing*. New York, NY: Springer (2010)
30. Liu Y, Sonek GJ, Berns MW, Tromberg BJ. Physiological monitoring of optically trapped cells: assessing the effects of confinement by 1064-nm laser tweezers using microfluorometry. *Biophys J* (1996) **71**(4):2158–67. doi:10.1016/s0006-3495(96)79417-1.
31. Shibata K. Spectrophotometry of intact biological materials. *J Biochem* (1958) **45**(8):599–623. doi:10.1093/oxfordjournals.jbchem.a126905.
32. Costantino AJ, Hyatt CJ, Kollisch-Singule MC, Beaumont J, Roth BJ, Pertsov AM. Determining the light scattering and absorption parameters from forward-directed flux measurements in cardiac tissue. *J Biomed Optic* (2017) **22**(7):76009. doi:10.1117/1.jbo.22.7.076009.
33. Goldsmith EC, Borg TK. The dynamic interaction of the extracellular matrix in cardiac remodeling. *J Card Fail* (2002) **8**(6):S314–S318. doi:10.1054/jcaf.2002.129258.
34. Longmore D. *Heart*. New York: NY: McGraw-Hill (1971)
35. Bugaisky LB, Zak R. Differentiation of adult rat cardiac myocytes in cell culture. *Circ Res* (1989) **64**(3):493–500. doi:10.1161/01.res.64.3.493.
36. Pirlo RK, Dean DMD, Knapp DR, Gao BZ. Cell deposition system based on laser guidance. *Biotechnol J* (2006) **1**:1007–13. doi:10.1002/biot.200600127.

Conflict of Interest: The authors declare that the research was conducted in the absence of any commercial or financial relationships that could be construed as a potential conflict of interest.